available at www.sciencedirect.com

ScienceDirect

journal homepage: www.elsevier.com/locate/ecolmodel

Study of the inter-annual food web dynamics in the Kuparuk River with a first-order approximation inverse model

Zhenwen Wan[a,b,*], *Joseph J. Vallino*[a], *Bruce J. Peterson*[a]

[a] *The Ecosystems Center, Marine Biological Laboratory, Woods Hole, MA 02543, USA*
[b] *State Key Laboratory of Marine Environmental Science, Xiamen University, Xiamen 361005, China*

ARTICLE INFO

Article history:
Received 16 January 2007
Received in revised form
21 August 2007
Accepted 24 August 2007
Published on line 29 October 2007

Keywords:
Inverse model
Ecosystem modeling
River ecosystem

ABSTRACT

We used a long-term observation data set (12 years) of fish, insect and primary producer standing stocks in both reference and phosphate-fertilized reaches of the Kuparuk River located on the north slope of Alaska, USA to test a recently developed first-order approximation model. The model employs a flow analysis-type approach, but uses first-order approximations between annual mean compartment stocks and environmental drivers of temperature, discharge and solar radiation. Consequently, the model is more robust and requires fewer observations than standard process-oriented models, and can utilize observations that are difficult to incorporate into process models. Unlike standard inverse models, we show that our model is capable of prediction provided sufficient data are available for model calibration and environmental drivers are known. The results show that the inter-annual variations of several components in the Kuparuk River ecosystem, including dissolve inorganic phosphate, chironomids, black flies and Arctic grayling, can be accurately approximated as a linear function of temperature, discharge and solar radiation. In particular, the model indicates that changes in river habitat brought about by proliferation of the moss *Hygrohypnum* spp. in the P-fertilized reach caused a temporary shift in flow paths supporting Arctic grayling from primary producers to detrital-based pathways. However, after moss establishment, primary producer flow paths to Arctic grayling returned and detrital-based pathways weakened.

1. Introduction

The Kuparuk River in Arctic Alaska is part of the Arctic Long-Term Ecological Research (LTER) site (http://ecosystems.mbl.edu/ARC/). One of the objectives of the Arctic LTER program is to predict how the ecosystem will respond to changes in environmental drivers that result from global change. Prediction is generally realized through detailed, process-oriented models where flows between trophic compartments are governed by mechanistic growth models that operate on short time scales (hours to days). This paper investigates the inter-annual dynamics using a recently developed first-order approximation model (Wan and Vallino, 2005, hereafter referred to as WV2005) that requires less information than conventional process-oriented models.

Starting in 1983, the Kuparuk River has been intensively investigated to study the long-term response of the river to phosphate enrichment. Over 30 papers have been published on the ecology of this fourth-order Arctic tundra stream. Most of these investigations have focused on the effects of

* *Corresponding author at*: State Key Laboratory of Marine Environmental Science, Xiamen University, Xiamen 361005, China. Tel.: +86 592 218 5510; fax: +86 592 218 0655.
E-mail address: zwan@xmu.edu.cn (Z. Wan).
0304-3800/$ – see front matter © 2007 Published by Elsevier B.V.
doi:10.1016/j.ecolmodel.2007.08.022

the long-term fertilization on separate trophic levels, including the effects on bacteria (Ford et al., 1989), *epilithic* diatom (Hullar and Vestal, 1989; Bowden et al., 1992; Miller et al., 1992; Peterson et al., 1993; Hershey et al., 1997; Harvey et al., 1998; Arscott et al., 1998), *bryophytes* (Bowden et al., 1994; Finlay and Bowden, 1994; Harvey et al., 1998; Arscott et al., 1998; Slavik et al., 2004), insects (Hiltner and Hershey, 1992; Hinterleitner-Anderson et al., 1992; Rublee and Partusch-Talley, 1995; Hershey et al., 1988, 1993; Harvey et al., 1998) and fish (Deegan and Peterson, 1992; Deegan et al., 1997, 1999; Harvey et al., 1998). Although these investigations greatly advanced our understanding of the system, the research followed a standard empirical three-step approach of observing, comparing and concluding. The standard three-step approach constitutes a first level analysis of the ecosystem and provides basic understanding of trophic interactions. However, because of the complexity of ecosystem processes, spatial heterogeneity, and fast dynamics, the three-step approach does not elucidate multiple or indirect interactions that can be very important. To account for these interactions, it is necessary to develop an ecosystem model. But the model must take into account that all processes active in an ecosystem may not be observable due to under sampling, lack of methods, or sampling methods that are difficult to incorporate into mathematical models.

In the case of the Kuparuk River, we have three challenges in developing a process-oriented model. First, some processes, which may significantly influence the ecosystem, have not yet been investigated thoroughly. For example, how discharge influences the sloughing process of the *epilithic* diatoms and the drift of insects is not well understood. A second concern is sampling frequency. We have nearly continuous information on some chemical and biological variables, but we lack continuous observations of microbes, moss, green filamentous algae, benthic detritus and particulate organic matter. Third, due to logistic difficulties, sampling schedules are sporadic, which means some ecosystem dynamics may not be captured by observations. Detailed process-oriented models describe the dynamics at all time scales, but they often focus on short time scales (hours to days) and therefore require high-frequency data for model validation. Since we are interested in long-term prediction, focusing instead on inter-annual cycles significantly reduces model complexity and data requirements.

Wan and Vallino (2005) formulated an inverse model with the following assumptions: (1) the long-term mean state of an ecosystem exists and is a basin of attraction provided environmental drivers stay within some boundaries, (2) the annual mean state is a minor bias from the long-term mean state, and (3) inter-annual dynamics linearly relate to the annual mean environmental drivers. Consequently, annual mean anomalies from long-term means for state variables can be approximated by linear responses of the environmental drivers annual mean anomalies from their long-term mean values. The first-order approximation of the ecosystem response to environmental drivers is able to describe the major inter-annual dynamics with yearly time resolution. This inverse model facilitates our primary objective of understanding ecosystem dynamics from available observations, but has the advantage that it can predict ecosystem state into the future given the appropriate environmental drivers. The modeling approach worked well with model generated observations and drivers (WV2005). This investigation of inter-annual dynamics in the Kuparuk River is the first application of the theoretical model with experimental observations.

The general implementation of the model is explained in WV2005, but is briefly summarized here. First, food web connectivity and the dependencies of each material flow must be specified (see Eqs. (25) and (29) in WV2005). For instance, in a standard NPZD model, N flows into P, which depends on N and P concentrations as well as temperature and light. Expert understanding of the ecosystem is critical to derive a conceptual model that accurately captures flow dependencies to at least first order. Because the conceptual model is based on a linear approximation, it can be inverted so that proportionality parameters can be derived from long-term means of observed state variables and environmental drivers and their annual mean deviations there from (e.g., Eqs. (30) and (31) in WV2005). Once model parameters are obtained from solution of the inverse problem, ecosystem responses can be forecasted provided environmental drivers with annual means are available for the period of interest (e.g., Eq. (32) of WV2005).

2. Site, food wed and measurement description

The upper Kuparuk River in Arctic Alaska is a fourth-order cobble bottom tundra river. It is studied as part of the Arctic LTER program and has been described previously (Kriet et al., 1992; Hershey et al., 1997; Wollheim et al., 1999; Slavik et al., 2004). In brief, the Kuparuk River originates in the foothills of Brooks Range, Alaska, U.S. and flows north to the Arctic Ocean. The intensively studied section of the river covers a 1.5 km fertilized reach and a 1.5 km reference reach. Since 1983, phosphate (P) has been added to the fertilized reach at a constant rate during the growing season (ca. 1 July–15 August) of each year to elevate P to approximately 0.3 μM above ambient levels at mean summer discharge (Slavik et al., 2004). The mean width in both reaches is approximately 17 m and the mean depth is approximately 0.4 m. Both reaches consist of 50% pool and 50% riffle runs (Wollheim et al., 1999).

The Kuparuk River ecosystem was previously grouped into 17 nitrogen compartments (Wollheim et al., 1999). This food web may be similarly represented with 17 phosphate compartments (Fig. 1), as phosphate is the limiting nutrient (Hullar and Vestal, 1988). The lower trophic level includes dissolved inorganic phosphate (DIP), dissolved organic phosphate (DOP), suspended particulate organic phosphate (SPOP), epilithic detritus (EDET) and benthic detritus (BDET). Primary producers include epilithic diatom (DIA), filamentous algae (ALG), moss (MOS), diatom growing on *Orthocladius*' feeding tube (T-D). Insects include *Baetis* (BAE), black flies (B-F), chironomids (CHI), *Brachycentrus* (BRA) and *Orthocladius* (ORT). The top consumers include *Rhyacophila* (RHY), young-of-the-year grayling (YOY) and adult grayling (A-G). The food web

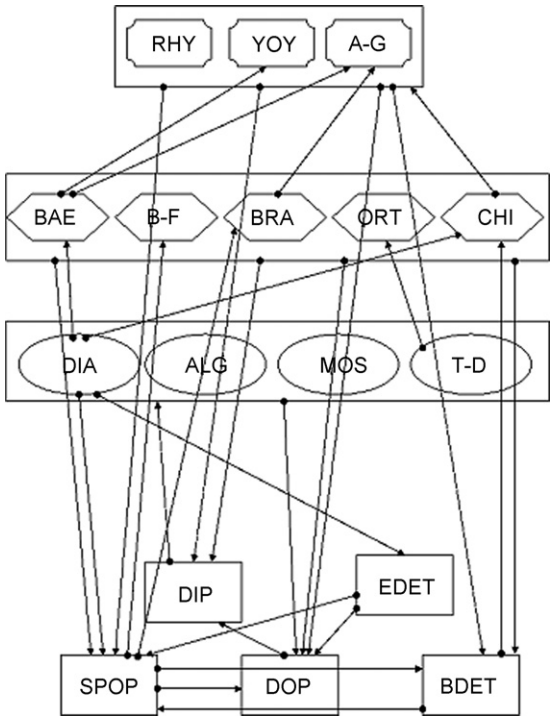

Fig. 1 – Kuparuk River food web based on observations. Abbreviations: DIP, dissolved inorganic phosphate; DOP, dissolved organic phosphate; SPOP, suspended particulate organic phosphate; EDET, epilithic detritus; BDET, benthic detritus; DIA, epilithic diatom; ALG, filamentous algae; MOS, moss; T-D, diatom growing on *Orthocladius*' feeding tube; BAE, *Baetis*; B-F, black flies; CHI, chironomids; BRA, *Brachycentrus*; ORT, *Orthocladius*; RHY, *Rhyacophila*; YOY, young-of-the-year graylings; A-G, adult graylings.

connections are summarized as follows: DIA is the primary food supplier to insect communities because ALG and MOS are not significantly grazed by insects. T-D is only grazed by ORT. BAE grazes DIA. CHI grazes both DIA and BDET. Both BRA and B-F feed on SPOP. Both YOY and A-G feed on BAE and CHI, but A-G also feeds on BRA. RHY feeds on CHI.

In the long-term fertilization experiment begun in 1983, DIP, DIA, BAE, CHI, BRA, B-F, ORT, RHY, YOY, A-G are measured almost every year, but measurements of DOP, BDET, EDET, SPOP, ALG, MOS and T-D are sporadic (Slavik et al., 2004). Flow analysis shows that DIA consumes 90% of DIP, while ALG, MOS and T-D consume the remaining 10% (Wollheim et al., 1999). Thus, we removed ALG, MOS and T-D from the food web since we do not have annual measurements. As ORT and RHY have low biomass, we ignored their influence on the food web. Because YOY and A-G have similar feeding characteristics, we aggregated them into a single fish compartment (FIS). Although we do not have annual measurements for SPOP, SPOP was found to correlate closely with discharge (Peterson et al., 1992). Discharge, temperature and solar radiation are continuously measured during the long-term experiment. Since we do not have annual data for DOP, BDET and EDET, we use a zero-order approximation to estimate their influence on the rest of the food web, by assuming they are constant. By definition, constant fluxes mean zero annual bias. The inter-annual dynamics in the first-order approximation inverse model are not influenced by fluxes with zero annual bias (WV2005). Therefore, when we remove DOP, BDET and EDET from the food web, it equates to taking a zero-order approximation, which in this case is the best estimation we can make without annual data, but this does not imply their connection to the food web does not exist. The above modifications resulted in a simplified food web (Fig. 2) that captures the main inter-annual phosphate dynamics in the Kuparuk River given our constraints on observations.

The simplified food web (Fig. 2) contains seven 'white compartments' (compartments which are annually observed), DIP, DIA, BAE, CHI, BRA, B-F, FIS, and two 'grey compartments' (compartments which are only sporadically observed), DOP and SPOP. Fluxes f_1, f_2, f_3, f_5, f_6, f_7, f_8, f_9, represent the major growth processes. Flux f_4 represents the sloughing process of DIA due to discharge that greatly impacts DIA dynamics (Wollheim et al., 1999). Fluxes f_{ia} ($i = 2, 3, 8, 9, 12$) represent animal waste production to DIP. Fluxes f_{ib} ($i = 1, 2, 3, 8, 9, 12$) represent animal waste production to DOP. Fluxes f_{ic} ($i = 2, 3, 8, 9, 12$) represent animal waste production to SPOP. Fluxes f_{10}, f_{11} and f_{13} represent the net advective transport of DIP, SPOP and DOP to the reach, respectively. Fluxes f_{Ta}, f_{Tb} and f_{Tc} stand for total annual waste production to DIP, DOP and SPOP, respectively.

3. The first-order approximation inverse model

We define the symbols $\hat{D}_{IP}$, $\hat{D}_{IA}$, $\hat{B}_{AE}$, $\hat{C}_{HI}$, $\hat{B}_{RA}$, $\hat{B}_{\text{-}F}$, $\hat{F}_{IS}$, $\hat{S}_{POP}$, $\hat{D}_{OP}$, $\hat{T}$, $\hat{L}$ and $\hat{D}$ to stand for the annual mean values of DIP, DIA, BAE, CHI, BRA, B-F, FIS, SPOP, DOP, temperature (T), light (L) and discharge (D), respectively. Similarly, $\bar{D}_{IP}$, $\bar{D}_{IA}$, $\bar{B}_{AE}$, $\bar{C}_{HI}$, $\bar{B}_{RA}$, $\bar{B}_{\text{-}F}$, $\bar{F}_{IS}$, $\bar{S}_{POP}$, $\bar{D}_{OP}$, $\bar{T}$, $\bar{L}$ and $\bar{D}$ stand for the long-term mean values and D'_{IP}, D'_{IA}, B'_{AE}, C'_{HI}, B'_{RA}, $B'_{\text{-}F}$, F'_{IS}, S'_{POP}, D'_{OP}, T', L', D' stand for the annual mean deviation from the long-term mean values, respectively. Hereafter, we generally use $\hat{X}$, $\bar{X}$, X' to stand for the annual mean, the long-term mean and the annual mean deviation from the long-term mean, respectively; $\hat{X} \equiv \bar{X} + X'$. To apply the first-order approximation inverse model, we must determine the primary dependencies of each flux based on our understanding of the ecosystem. Flux f_1 characterizes the nutrient uptake process of the epilithic diatom. The direct dependences of f_1 are assumed to include DIP, DIA, T and L. Flux f_2 characterizes *Baetis* feeding on epilithic diatom, so includes dependencies on DIA, BAE, T and D. Flux f_3 characterizes chironomids feeding on epilithic diatoms, which depends on DIA, CHI, T and D. Flux f_4 characterizes epilithic diatom sloughing to SPOP, so depends on DIA and D. Flux f_5 characterizes fish feeding on BAE, which depends on BAE, FIS, T and D. Flux f_6 characterizes fish feeding on CHI, which depends on CHI, FIS, T and D. Flux f_7 characterizes fish feeding on BRA, which depends on BRA, FIS, T and D. Flux f_8 stands for *Brachycentrus* filtering of SPOP, so depends on BRA, T and D, since SPOP is a function of D. Flux f_9 characterizes black flies filtering of SPOP, which depends on B-F, T and D. Based on these assumptions, the annual mean deviations of the major fluxes

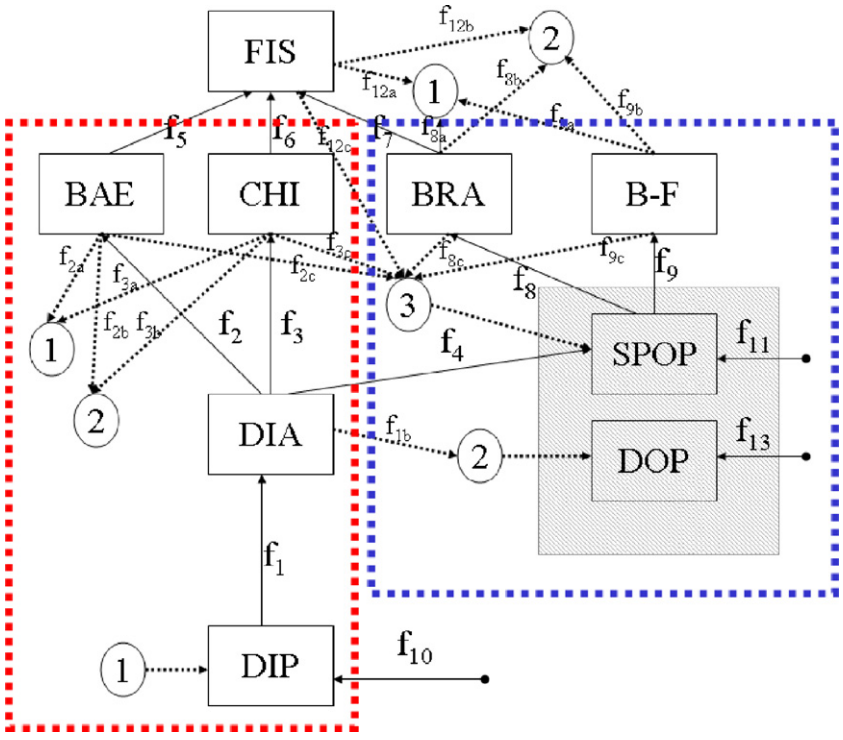

Fig. 2 – Simplified food web used to model Kuparuk River consisting of seven 'white' compartments and two 'grey' compartments. Abbreviations: FIS, both young and adult graylings; other symbols are same as in the caption of Fig. 1. Circled numbers 1–3 represent connections to DIP, DOP, and SPOP, respectively. The red box indicates autotrophic-based support of FIS, while the blue box highlights detrital-based support of FIS. (For interpretation of the references to colour in this figure legend, the reader is referred to the web version of the article.)

f_1–f_9 from their long-term mean values may be expressed, following Eqs. (25) and (28) in WV2005, as

$$f_1' = c_{11}D_{IP}' + c_{12}D_{IA}' + c_{13}\frac{\bar{D}_{IP}}{\bar{T}}T' + c_{14}\frac{\bar{D}_{IP}}{\bar{L}}L',$$

$$f_2' = c_{21}D_{IA}' + c_{22}B_{AE}' + c_{23}\frac{\bar{D}_{IA}}{\bar{T}}T' - c_{24}\frac{\bar{D}_{IA}}{\bar{D}}D',$$

$$f_3' = c_{31}D_{IA}' + c_{32}C_{HI}' + c_{33}\frac{\bar{D}_{IA}}{\bar{T}}T' - c_{34}\frac{\bar{D}_{IA}}{\bar{D}}D',$$

$$f_4' = c_{41}D_{IA}' + c_{42}\frac{\bar{D}_{IA}}{\bar{D}}D',$$

$$f_5' = c_{51}B_{AE}' + c_{52}F_{IS}' + c_{53}\frac{\bar{B}_{AE}}{\bar{T}}T' + c_{54}\frac{\bar{B}_{AE}}{\bar{D}}D',$$

$$f_6' = c_{61}C_{HI}' + c_{62}F_{IS}' + c_{63}\frac{\bar{C}_{HI}}{\bar{T}}T' + c_{64}\frac{\bar{C}_{HI}}{\bar{D}}D',$$

$$f_7' = c_{71}B_{RA}' + c_{72}F_{IS}' + c_{73}\frac{\bar{B}_{RA}}{\bar{T}}T' + c_{74}\frac{\bar{B}_{RA}}{\bar{D}}D',$$

$$f_8' = c_{81}B_{RA}' + c_{82}\frac{\bar{B}_{RA}}{\bar{T}}T' + c_{83}\frac{\bar{B}_{RA}}{\bar{D}}D',$$

$$f_9' = c_{91}B_{-F}' + c_{92}\frac{\bar{B}_{-F}}{\bar{T}}T' + c_{93}\frac{\bar{B}_{-F}}{\bar{D}}D', \qquad f_{10}' = c_{101}\frac{\bar{D}_{IP}}{\bar{D}}D' \tag{1}$$

where c_{ij} (i, j = 1, 2, …, 10) are model parameters. In addition, we assume production linearly correlates with consumption, which may be expressed as

$$\frac{f_{2a}}{f_2} = \frac{f_{3a}}{f_3} = \frac{f_{8a}}{f_8} = \frac{f_{9a}}{f_9} = \frac{f_{12a}}{f_{12}} = c_a,$$

$$\frac{f_{2b}}{f_2} = \frac{f_{3b}}{f_3} = \frac{f_{8b}}{f_8} = \frac{f_{9b}}{f_9} = \frac{f_{12b}}{f_{12}} = c_b,$$

$$\frac{f_{2c}}{f_2} = \frac{f_{3c}}{f_3} = \frac{f_{8c}}{f_8} = \frac{f_{9c}}{f_9} = \frac{f_{12c}}{f_{12}} = c_c, \qquad f_{12} = f_5 + f_6 + f_7 \tag{2}$$

where c_a, c_b and c_c stand for animal DIP, DOP and SPOP waste-to-consumption ratios, respectively. According to the food web connectivity (Fig. 2), the first-order approximation inverse model may be written, following Eq. (29) in WV2005, as

$$\begin{pmatrix} -1 & \alpha & \alpha & 0 & \alpha & \alpha & \alpha & \alpha & \alpha & 1 \\ \beta & -1 & -1 & -1 & 0 & 0 & 0 & 0 & 0 & 0 \\ 0 & \gamma & 0 & 0 & -1 & 0 & 0 & 0 & 0 & 0 \\ 0 & 0 & \gamma & 0 & 0 & -1 & 0 & 0 & 0 & 0 \\ 0 & 0 & 0 & 0 & 0 & 0 & -1 & \gamma & 0 & 0 \\ 0 & 0 & 0 & 0 & 0 & 0 & 0 & 0 & \gamma & 0 \\ 0 & 0 & 0 & 0 & \gamma & \gamma & \gamma & 0 & 0 & 0 \end{pmatrix} \begin{pmatrix} f_1' \\ f_2' \\ f_3' \\ f_4' \\ f_5' \\ f_6' \\ f_7' \\ f_8' \\ f_9' \\ f_{10}' \end{pmatrix} = \begin{pmatrix} D_{IP}' \\ D_{IA}' \\ B_{AE}' \\ C_{HI}' \\ B_{RA}' \\ B_{-F}' \\ F_{IS}' \end{pmatrix} \tag{3}$$

where $\alpha = c_a$, $\beta = 1 - c_b$ and $\nu = 1 - c_a - c_b - c_c$. Replacing f_i' ($i = 1, 2, \ldots, 10$) in Eq. (3) with Eq. (1), we can formulate a linear matrix equation (Eq. (A1), Appendix A) with respect to the unknown first-order approximation model parameters, c_{ij}. Once the unknowns, c_{ij}, are determined from available data, Eq. (A1) is converted to a prediction model with respect to unknowns, D'_{IP}, D'_{IA}, B'_{AE}, C'_{HI}, B'_{RA}, B'_{-F} and F'_{IS} (Eq. (A2), Appendix A).

4. Data

The Kuparuk River is located within the Arctic Circle (68°38′N, 149°24′W). It is completely frozen from October to May, with the growing season from early June to late August. Thus, the annual mean concentrations are defined as the average over the growing season. The annual mean values were derived from field measurements in summer (Slavik et al., 2004). The data used for model development and calibration include the drivers of temperature, T (°C), light intensity, L (W m^{-2}), and discharge, D (m^3 s^{-1}), as well as observations of DIP (μg P L^{-1}), DIA (μg Chl cm^{-2}), insect (BAE, CHI, BRA, B-F) densities (abundance m^{-2}) and A-G and YOY annual weight increment (g day^{-1}). Although the original data have different units, they were converted into area-specific phosphate concentrations (mmol P m^{-2}). DIP, DIA, insect density and fish weight increments were converted into area-specific N concentrations with the conversion factors given by Wollheim et al. (1999, Table 1), then converted to P concentrations with conversion factor of N:P = 16. The area-specific P concentrations from Slavik et al. (2004) represent the organism concentration averaged over the habitat area where the organisms are found; they are not averaged over the entire reach. Consequently, the habitat area must be approximated to obtain area-specific concentrations based on the entire reach. This is particularly important for organisms that utilize the moss habitat, since the moss coverage in the riffle sections of the fertilized reach increases with time. Based on observations, the moss coverage is relatively constant at 5% in the reference reach, while the coverage increases from 5% in 1988 to 50% in 1992 and remains constant at 50% after 1992 in the fertilized reach. We approximate the fractional habitat areas for DIA, CHI, BRA, BAE and B-F, as (1–0.5r_M), 0.5r_M, 1.0, 0.5(1 − r_M), 0.5(1 − r_M) and 1.0, respectively, where r_M stands for moss coverage fraction and the 0.5 factor reflects that only 50% of the reach is riffle habitat. The area-specific P concentration from Slavik et al. (2004) multiplied by the fractional habitat area gives the average P concentration over the reach. The data for annual mean environmental drivers (T, L and D) are shown in Fig. 3. The data of annual mean area-specific P concentration for each food web compartment for the reference and fertilized reaches are shown in Fig. 4.

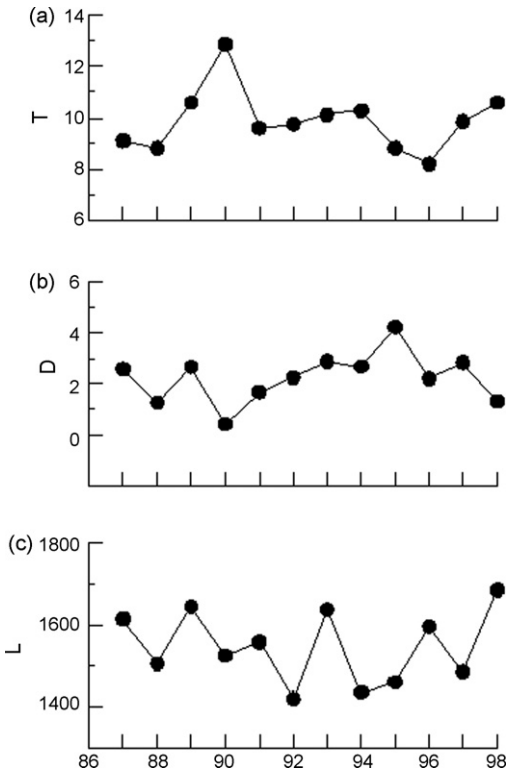

Fig. 3 – Observed annual mean environmental drivers for years 1987–1998 for: (a) temperature, T (°C); (b) discharge, D (m^3 s^{-1}); (c) solar radiation, L (W cm^{-2}).

5. Results and discussion

5.1. *Case 1: hindcast using complete 12 years of data to determine model parameters*

There are 12 years of data (Figs. 3 and 4) for the reference and fertilized reaches of the Kuparuk River. The equation set (Eq. (A1)) exists for each year. Thus there are 84 linear equations for 33 unknowns (c_{ij}). We preset relative waste production constants c_a, c_b and c_c to 0.1, 0.1 and 0.3, respectively (Wollheim et al., 1999). The over-determined linear equation set is converted into a well-determined equation set under a least-squares constraint. The well-determined equation set is solved for the 33 unknowns (c_{ij}) through Gauss-Seidel iteration.

The solution of unknowns (c_{ij}) are listed in Table 1 as *Case 1R* for the reference reach and *Case 1F* for the fertilized reach. Eq. (A2) is used to predict the inter-annual dynamics of D'_{IP}, D'_{IA}, B'_{AE}, C'_{HI}, B'_{RA}, B'_{-F} and F'_{IS} using the solved unknowns (c_{ij}), the long-term means, $\bar{D}_{IP}$, $\bar{D}_{IA}$, $\bar{B}_{AE}$, $\bar{C}_{HI}$, $\bar{B}_{RA}$, $\bar{B}_{-F}$, $\bar{F}_{IS}$, $\bar{T}$, $\bar{L}$, $\bar{D}$ and environmental drivers, T', L' and D'. We refer to this prediction as a *hindcast*, because we used all 12 years of data to determine the model parameters (c_{ij}). The comparison of the model with the data is plotted in Figs. 5 and 6 for the reference and fertilized reaches, respectively. Overall, the predicted results reproduce the trends of inter-annual dynamics exhibited by the observations, especially for compartments DIP, CHI, B-F and FIS in both reaches. In particular, DIP has a continuous increment from 1987 to 1990 followed by a continuous decrement to 1996, which the model reproduces (Fig. 6a). CHI drops from 1987 to 1989 and then continuously climbs until 1997, which the model captures well except for in 1989, 1991 and 1997 (Fig. 6d). The model exhibits good skill for both B-F (Figs. 5f and 6f) and FIS (Figs. 5g and 6g) in both reaches. For DIA in both reaches (Figs. 5b and 6b), the observations exhibit

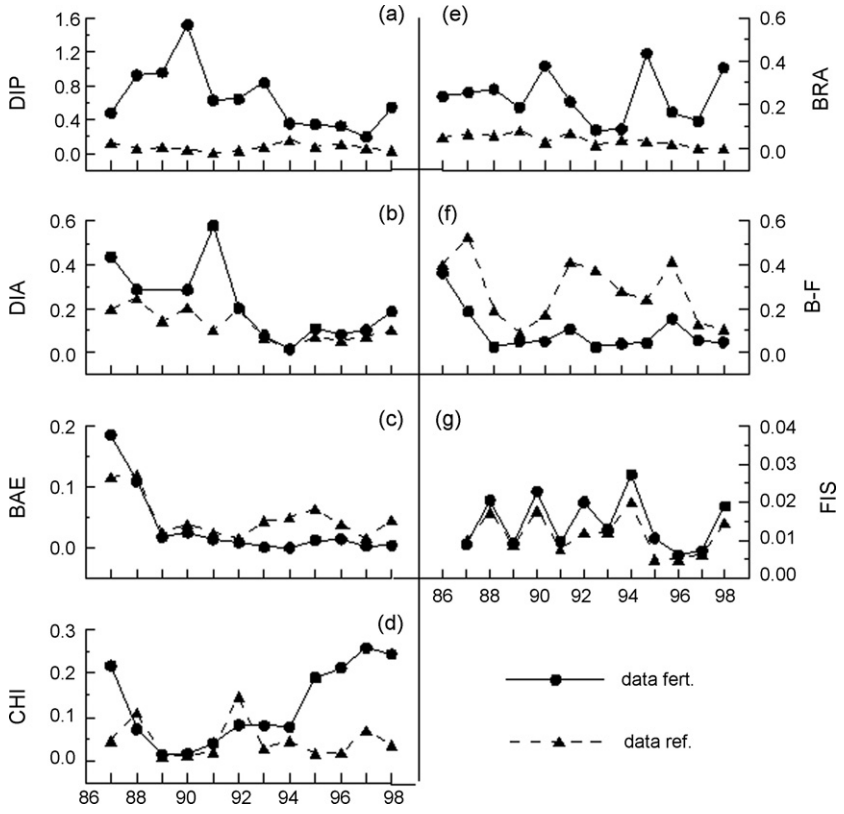

Fig. 4 – Annual mean observations from 1987 to 1998 used for model calibration and forecasting. Filled circles are observations in fertilized reach and triangles for observations in the reference reach. All observations have been converted to mmol P m^{-2}.

a general decreasing trend with time, which the model also captures. We speculate that the poor model fit to BRA observations is a result of BRAs lifecycle, which is longer than 1 year. However, the modeling approach of WV2005 pertains to organisms whose lifecycles are shorter than 1 year. Annual growth increments can be used for organisms with lifecycles greater than 1 year, as was done for FIS, but this was not implemented for BRA. The factors causing poor model fit to BAE remain uncertain; however, changes in BAEs physical habitat as a result of changes in moss coverage that were not captured

Table 1 – Parameter values, c_{ij}, of the first-order approximation model obtained from data assimilation

Case	c_{11}	c_{12}	c_{13}	c_{14}	c_{21}	c_{22}	c_{23}	c_{24}	c_{31}	c_{32}	c_{33}
1R	−0.58	0.13	−0.10	−1.77	0.10	−0.22	−0.26	−0.16	0.10	0.12	0.24
2R	−0.75	0.16	−1.05	2.56	0.03	−0.67	−1.41	−0.04	−0.01	−0.28	−0.40
1F	−0.65	−0.15	−1.12	2.11	0.06	−0.99	−5.95	−0.43	−0.03	1.43	1.19
2F	−0.53	−0.16	−1.78	2.81	0.05	−0.90	−6.85	−0.47	−0.04	1.26	1.22
Case	c_{34}	c_{41}	c_{42}	c_{51}	c_{52}	c_{53}	c_{54}	c_{61}	c_{62}	c_{63}	c_{64}
1R	−0.12	−0.97	−0.38	−0.93	0.73	−0.08	0.25	−0.79	0.91	0.37	0.22
2R	0.13	−0.63	−0.09	−1.20	1.01	−1.43	0.18	−1.11	1.37	0.58	0.02
1F	−0.18	−1.10	−0.04	−1.13	−0.36	−20.9	2.08	−0.24	0.53	1.26	0.20
2F	−0.21	−1.07	−0.12	−1.11	−0.56	−23.9	2.35	−0.21	0.45	1.60	0.20
Case	c_{71}	c_{72}	c_{73}	c_{74}	c_{81}	c_{82}	c_{83}	c_{91}	c_{92}	c_{93}	c_{101}
1R	0.80	1.56	−7.77	−1.28	3.71	−14.5	−2.86	1.05	−0.10	−0.04	0.21
2R	1.56	1.51	−12.6	−1.52	5.19	−24.7	−3.38	1.02	−0.10	−0.04	0.33
1F	−0.10	0.16	1.02	−0.63	1.76	2.03	−1.27	1.00	−0.05	−0.03	−0.08
2F	−0.13	−0.50	0.75	−0.75	1.77	1.48	−1.48	1.00	−0.05	−0.04	−0.06

All units are in $year^{-1}$.

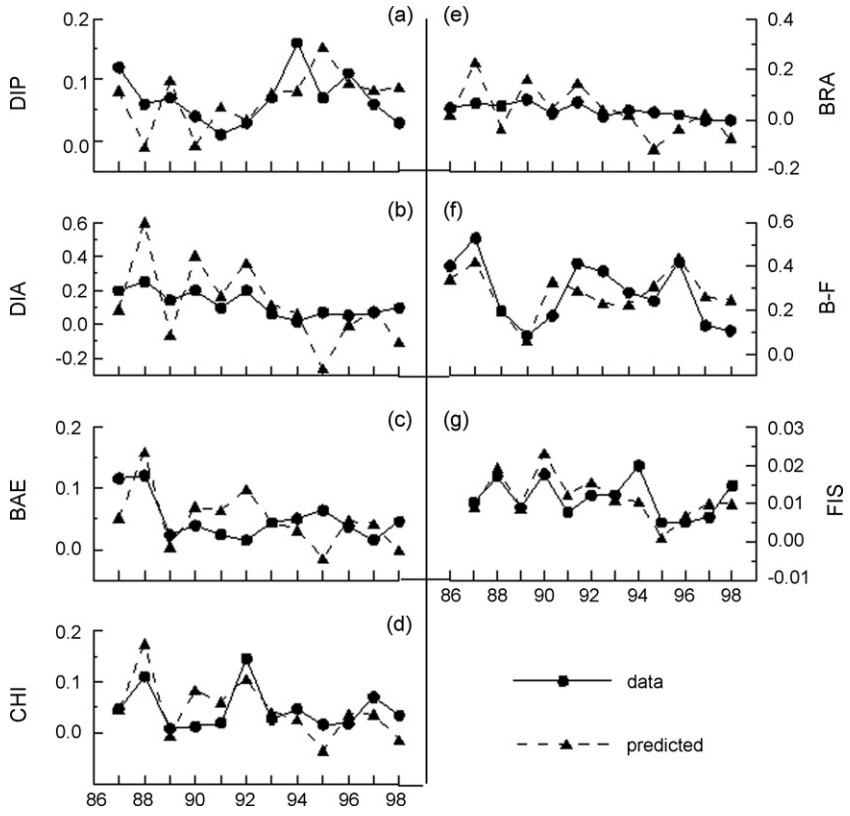

Fig. 5 – Comparison of model predictions (filled triangles) to observations (filled circles) in the reference reach for Case 1R; all observations used in model fit. Units are in mmol P m^{-2}.

accurately with observations is a likely cause (Slavik et al., 2004).

To quantify model fit to observations, we use the modified index of agreement, d_1, as defined by Legates and Mccabe (1999). The index of agreement varies between 0 and 1 and is a measure of the mean error versus the potential error, with higher values representing better model fits. The indices of agreement are listed in Table 2a for *Case 1R* (reference reach) and *Case 1F* (fertilized reach). In brief, the prediction captures the observed inter-annual dynamics pattern, with d_1 indices of ca. 0.4 in the reference reach and ca. 0.6 in the fertilized reach. The predicted curves match the observed values for DIP, CHI, B-F and FIS, with d_1 values of 0.43, 0.47, 0.59 and 0.55 in reference reach and 0.62, 0.63, 0.60 and 0.59 in fertilized reach, respectively. The prediction also reflects the general dynamics for DIA, BAE, and BRA. In brief, these results show that the first-order approximation model is able to capture the dynamics of the true ecosystems in hindcast mode.

5.2. *Case 2: forecast using 9 years of data to determine model parameters*

For the above hindcast cases, all 12 years of data were used to determine the first-order approximation model parameters. As there are 33 parameters, 5 years of data are theoretically sufficient to determine all model parameters. However, due to observational errors, 5 years of data do not provide enough resolution of model parameters. In order to obtain a good fit between model and observations, we found that 9 or more years of data were required for parameter estimation. Referred to as *Case 2*, the simulated results for the first 9 years is the hindcast where the data are used to estimate model parameters (c_{ij}), while the remaining 3 years of simulation can be considered a forecast, as these data were not used in parameter estimation.

Model parameters, c_{ij}, using the first 9 years of data are referred to as *Cases 2R* and *2F* for the reference and fertilized reaches, respectively (Table 1). The indices of agreement, d_1, for *Case 2* are separated into hindcast for the first 9 years

Table 2a – The index of agreement of the hindcasted model

Case	DIP	DIA	BAE	CHI	BRA	B-F	FIS
1R	0.43	0.30	0.40	0.47	0.25	0.59	0.55
2R	0.41	0.29	0.42	0.50	0.20	0.59	0.53
1F	0.62	0.49	0.54	0.63	0.53	0.60	0.59
2F	0.64	0.48	0.58	0.56	0.54	0.60	0.61

Table 2b – The index of agreement of the forecasted model

Case	DIP	DIA	BAE	CHI	BRA	B-F	FIS
2R	0.47	0.15	0.29	0.37	0.17	0.58	0.54
2F	0.40	0.32	0.15	0.20	0.50	0.58	0.49

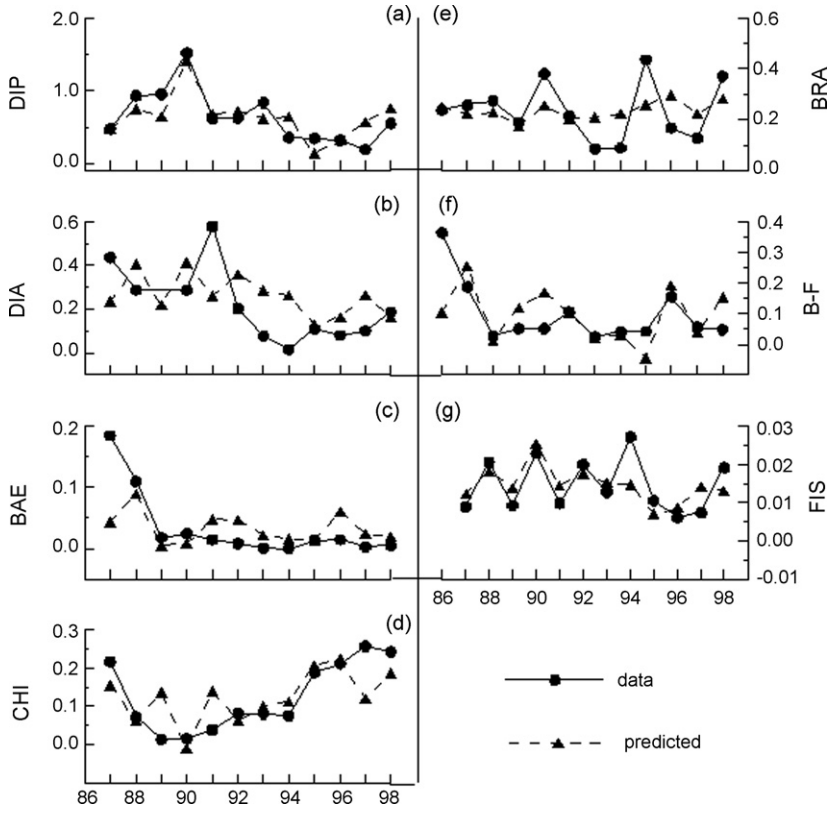

Fig. 6 – Comparison of model predictions (filled triangles) to observations (filled circles) in the fertilized reach for Case 1F; all observations used in model fit. Units are in mmol P m^{-2}.

(Table 2a) and forecast for the remaining 3 years (Table 2b). As can be seen from *Case 1F* versus *Case 2F* (Figs. 6 and 8), there are no significant differences between the predicted results using 9 years of data versus 12 years of data, except for BRA. The model parameters for Cases *1F* and *2F* are also similar, except for parameter c_{72} (Table 1). Thus, 9 years of data are sufficient to parameterize the model for the fertilized reach. Since the parameters are similar for the two cases in the fertilized reach, the forecast results in the remaining 3 years are similar to the hindcast results in *Case 1F*. Although the forecasted results are not perfect, the results illustrate that the modeling approach has the capability of forecasting. The forecast matches the observations for DIP in 1996 and 1998, and similar fits occur for DIA in 1997, for BAE in 1997 and 1998, for CHI in 1996, for BRA in 1997, for B-F in 1996 and 1997 (Fig. 8).

Comparing the results from *Case 1R* and *Case 2R* (Figs. 5 and 7), we see the two predicted curves have similar patterns, but there are some differences. Many of the model parameters are also different (Table 1). It appears that the parameters for the reference reach model are not fully resolved with 9 years of data. This parameter resolution problem may be due to the very low levels of SRP and chlorophyll in the Kuparuk River, with the latter often being below the limits of detection (Slavik et al., 2004). As a result, signal-to-noise ratio in the reference reach is higher than in the fertilized reach, making parameter estimation and model identification more difficult.

Considering all four cases, it is apparent that prediction for DIP, CHI, B-F and FIS are more accurate than for DIA, BAE and BRA and prediction is better for the fertilized reach than the reference reach. Three aspects potentially influence prediction accuracy. First, there exist nonlinear ecological dynamics, which cannot be represented by the first-order approximation model. Second, the food web (Fig. 2) does not directly include moss. Because there were insufficient observations for moss coverage, we used moss coverage as another environmental driver instead of a state variable. Although moss in the reference reach has low nutrient consumption (Wollheim et al., 1999), moss competes with epilithic diatoms for space and greatly influences insect habitat, especially in the fertilized reach. Third, this approximation model was developed to simulate a mature ecosystem; that is, we assume that internal dynamics have dissipated and the ecosystem tracks environmental drivers (van den Berg, 1998; WV2005). The fertilized reach of the Kuparuk River should not be regarded as a typical mature ecosystem, because the long-term fertilization introduces a transient in the first 4 years as moss coverage increases from 5% to 50% (Slavik et al., 2004).

5.3. *Influence of long-term fertilization on ecological dynamics*

Below we compare the inter-annual variations of stocks between the reference and fertilized reaches using predicted fluxes (Figs. 9 and 10, respectively). The analysis is focused on distinguishing natural changes from fertilization-influence changes. This analysis reveals some interesting ecological dynamics influenced by the long-term fertilization. It is impor-

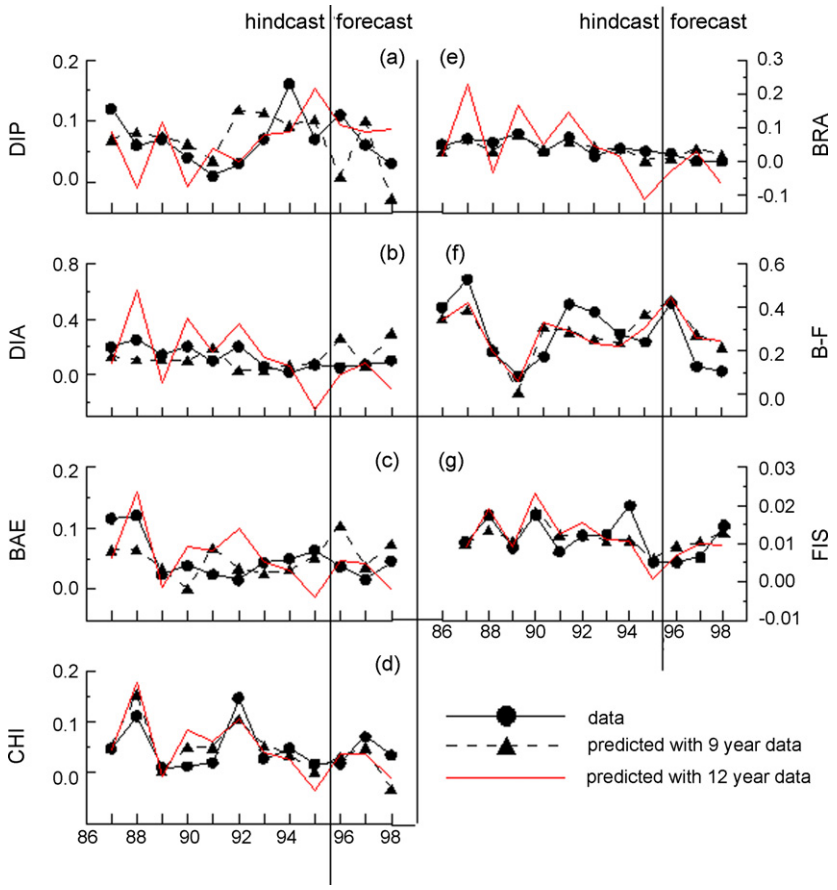

Fig. 7 – Comparison of model predictions (filled triangles) with observations (filled circles) in the reference reach for Case 2R; only first 9 years of data used in model fit. Years 1996–1998 are model forecasts. Solid line is model results from Fig. 5. Units are in mmol P m^{-2}.

tant to recall, however, that these fluxes (f') represent mean annual *deviations* from the long-term mean fluxes (i.e., $f' = \hat{f} - \bar{f}$). Consequently, a negative flux value does not mean that the overall flux between compartments is flowing in the opposite direction, but rather that the flux is less than the long-term mean. Since the long-term mean flux ($\bar{f}$) is unknown, the modeling approach does not allow determination of the annual mean flux ($\hat{f}$) (see WV2005). It is also important to consider the observed influence of long-term fertilization in Kuparuk River detailed by Slavik et al. (2004), which we briefly summarize here. Long-term fertilization produced positive responses for all trophic levels from primary producers to fish, but negative responses for BAE and B-F. While the fertilization began in 1983, radical change in community structure did not occur until the development of the moss *Hygrohypnum*, which nearly completely covered the stream bottom in riffle habitats starting abruptly in 1992.

5.3.1. *DIP dynamics*

The inter-annual variation of DIP relates to the dynamics of DIA uptake (f_1) without significant influence from DIP input (f_{10}) (Figs. 9a and 10a), since little phosphate enters from lateral seepage in the reference reach and P-addition occurred at a constant rate in the fertilization reach (Slavik et al., 2004). This indicates that the inter-annual variation of the area-specific phosphate concentration is mainly caused by local biology, with dominance between DIP uptake (f_1) and DIP remineralization (f_{Ta}) changing from one year to the next. Although the moss increase is a major response to the long-term fertilization, the inter-annual variation of DIP caused by moss uptake is not significant enough to cause the inter-annual variation in DIP stock (Slavik et al., 2004). Apparently, either DIP consumption by moss is similar to that of DIA, or DIP moss consumption does not have significant inter-annual variation. However, we note that DIA was measured attached to bare rocks only while epiphyte growth on moss was not readily measurable. Since the moss coverage had a significant increase in 1992–1993, the noticeable drop in DIP since 1994 (Fig. 6a) may be explained by a corresponding jump in epiphytic DIA that went unmeasured. In contrast, the model result for DIP in the reference reach (Fig. 5a) reflects the dominant impact from DIA (Fig. 5b), which exhibits the expected inverse response between DIP and DIA.

5.3.2. *DIA dynamics*

In the reference reach, the DIA sloughing process (f_4) is the main cause of the inter-annual variation of DIA (Fig. 9b). In the fertilized reach, all fluxes (f_1–f_4) have significant influence on DIA (Fig. 10b), but DIA sloughing (f_4) is still dominant. The fertilization causes greater variation of DIP uptake (f_1),

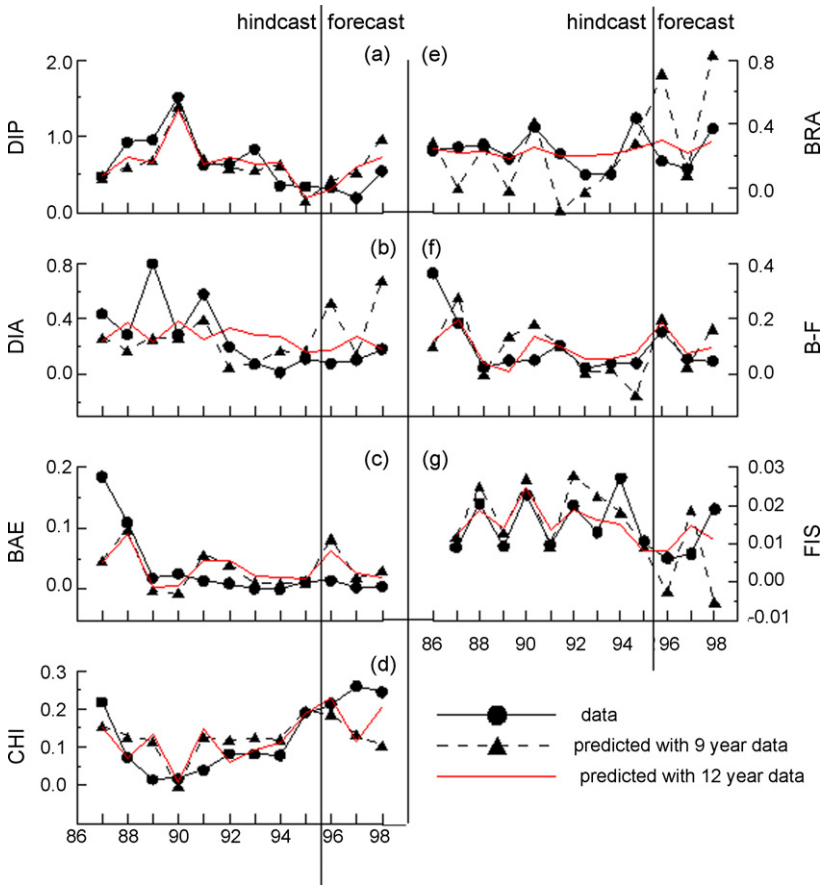

Fig. 8 – Comparison of model predictions (filled triangles) with observations (filled circles) in the fertilized reach for Case 2F; only first 9 years of data used in model fit. Years 1996–1998 are model forecasts. Solid line is model results from Fig. 6. Units are in mmol P m^{-2}.

whose dynamics are passed onto upper trophic levels. The reason why the inter-annual dynamics of DIA (Fig. 6b) does not reflect the impact of DIP (Fig. 6a) is explained above. The model reproduces well the year-to-year changes of observed DIA in reference reach except in 1995 and 1998 (Fig. 5b). It appears that fertilization stimulates DIA growth and the insects feeding on DIA, which is consistent with the increase in NH_4^+ uptake in the fertilized reach observed during a ^{15}N trace addition study (Wollheim et al., 2001).

5.3.3. *BAE dynamics*

In the reference reach, fluxes f_2 and f_5 exhibit similar year-to-year variations (Fig. 9c), which indicates that the contribution of BAE to FIS is controlled by the production of BAE. This is consistent with model results for DIA and BAE (Fig. 5b and c), which show similar year-to-year changes in DIA and BAE. The year-to-year changes of DIA are similar in both reaches after 1992 (Fig. 4b), but BAE in the fertilized reach has a relatively lower stock than in the reference reach after 1992 (Fig. 4c), indicating a greater top-down control in the fertilized reach. However, moss also provides poor habitat for BAE as well. Considering fluxes in the fertilized reach, the consumption (f_2) and production (f_5) of BAE are balanced (Fig. 10c); consequently, BAE density remains constant. In fact, BAE contributed more to FIS after 1992, as evident by f_5 in Fig. 10g. Fish appear to rapidly change their BAE feeding rate (or preference) in response to changes in BAE growth rate in the fertilized reach. As the moss coverage in the fertilized reach became significant 1992, it is possible that the long filamentous moss made BAE more susceptible to fish grazing due to changes in streambed hydrodynamics (Wetmore et al., 1990).

5.3.4. *CHI dynamics*

Both CHI growth (f_3) and predation (f_6) have significant influence on the inter-annual variation of CHI in both reaches, but FIS predation (f_6) has more influence in the reference reach while CHI growth (f_3) has more influence in the fertilized reach (Figs. 9d and 10d). Consequently, CHI density exhibits top–down control in the reference reach, but bottom–up control in the fertilized reach. The high abundance of CHI in the fertilized reach after 1994 (Fig. 4d) comes from increased CHI growth (Fig. 10d). Although CHI consumes resources from both DIA and BDET (Fig. 1), observations indicate higher BDET concentrations trapped within the moss, which should stimulate CHI growth. Nevertheless, it appears that the zero-order approximation for the benthic detritus (BDET) is justified, as the predicted CHI density matches the data well (Fig. 6d). While the stock of epilithic DIA dropped after 1991, this does not indicate that total DIA production decreased (Slavik et al., 2004). As moss cover became established in 1992, moss epi-

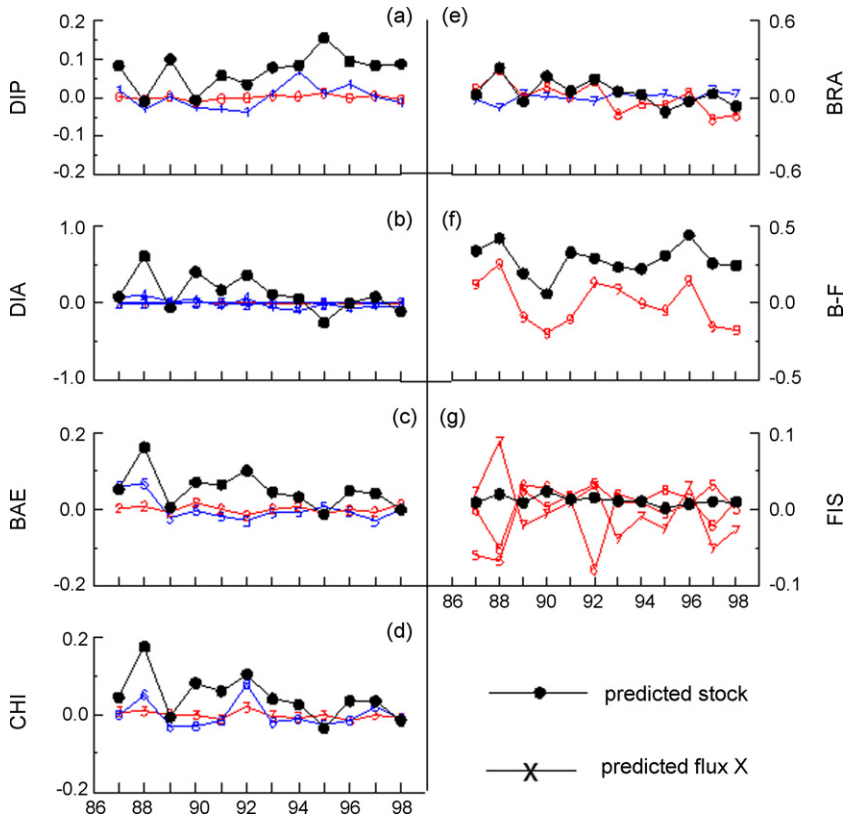

Fig. 9 – Comparison of stock inter-annual variations (filled circles, mmol P m^{-2}) with associated input–output fluxes (mmol P m^{-2} $year^{-1}$) for the reference reach. Numbers and lines refer to fluxes shown in Fig. 2 and Eq. (1), where red indicates in-flow and blue out-flow (*note*, sign on out-flowing fluxes have been reversed). (For interpretation of the references to colour in this figure legend, the reader is referred to the web version of the article.)

phytic DIA became an additional food for CHI and this fraction of DIA was not measured nor calculated as discussed above. The same rational explains why BRA in the fertilization reach did not decrease obviously after 1992. The good model-data-fit for CHI in the reference reach (Fig. 5d) reflects that the CHI abundance is impacted by DIA availability. In the reference reach, the model results for BAE, CHI and BRA have same pattern as that for DIA. This indicates that the food availability is a dominant factor controlling insect abundance; however, habitat is also an important factor.

5.3.5. *BRA dynamics*

In both reaches, BRA prediction does not match the observations well, in that predictions are either too dynamic (reference reach, Fig. 5e) or lack dynamics (fertilized reach, Fig. 6e). In the reference reach, BRA predation (f_7) and feeding (f_8) fluxes have low amplitude dynamics, but are asynchronous, so that predicted BRA densities fluctuate (Fig. 9e). Conversely, the same fluxes have large amplitude dynamics in the fertilized reach, but are synchronous, so that BRA densities remain flat. The reasons for the poor BRA predictions remain unclear. However, BRA is the only insect with a 3-year life cycle and the inter-annual biomass accumulation violates an assumption of the first-order approximation model, which requires that each ecosystem state variable be independent of the previous year unless annual growth increments are used as observations (WV2005).

5.3.6. *B-F dynamics*

Predicted B-F densities match the observations well for both the reference and fertilized reaches (Figs. 5f and 6f, respectively). Feeding rate (f_9) controls B-F dynamics, since mortality is assumed proportional to feeding (Eq. (2)). B-F consumes SPOP, which correlates strongly to discharge (Peterson et al., 1992), but temperature (Fig. 3b) influences feeding dynamics (f_9) (Figs. 9f and 10f), as evident by the magnitude of parameter c_{92} (Table 1). Comparison of T and D (Fig. 3) and f_9 indicates discharge dominates B-F abundance. However, fertilization did not alter SPOP availability, but the increase in BRA resulting from fertilization displaced B-F from its habitat. Furthermore, B-F prefers bare rock habitats to moss or biofilm covered rock habitats. The larger prediction error in the fertilized reach between 1990 and 1992 (Fig. 6f) likely reflects the transient period when moss coverage rapidly increased.

5.3.7. *FIS dynamics*

The predicted FIS annual biomass increment (or growth) matches the observations well for both reaches (Figs. 5g and 6g). FIS prey has comparatively large amplitude dynamics, but FIS annual increment tends to be relatively constant. This implies that environmental drivers rather than

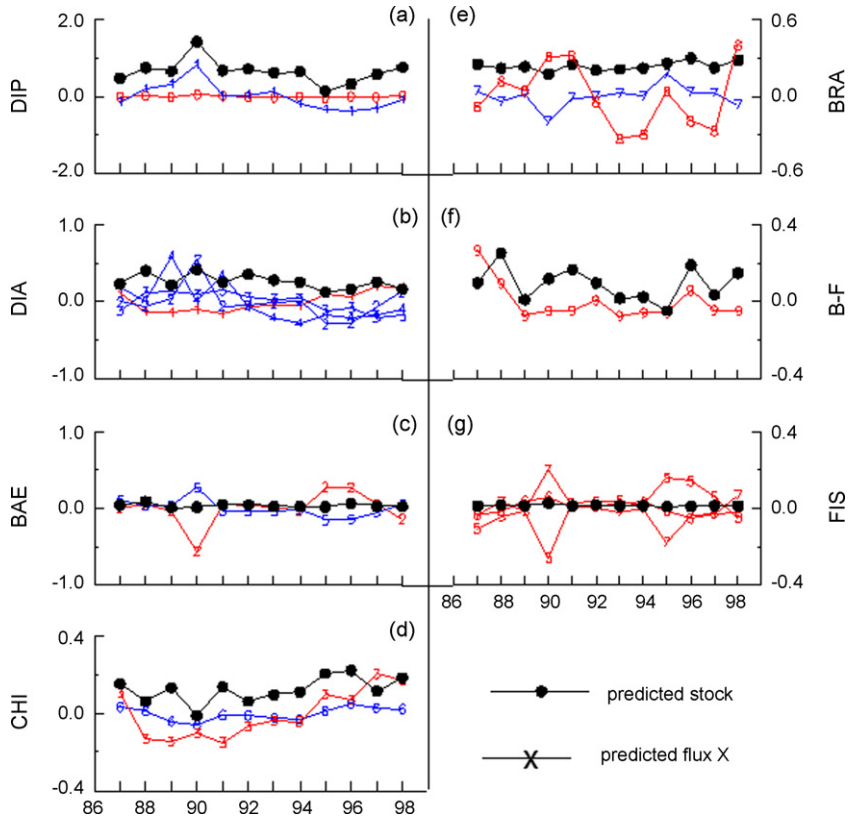

Fig. 10 – Comparison of stock inter-annual variations (filled circles, mmol P m^{-2}) with associated input–output fluxes (mmol P m^{-2} $year^{-1}$) for the fertilized reach. Numbers and lines refer to fluxes shown in Fig. 2 and Eq. (1), where red indicates in-flow and blue out-flow (note, sign on out-flowing fluxes have been reversed). (For interpretation of the references to colour in this figure legend, the reader is referred to the web version of the article.)

prey density may govern FIS dynamics, which is consistent with the large model coefficients associated with T' and D' (c_{53}, c_{54}, c_{63}, c_{64}, c_{73}, and c_{74}, Table 1). The patterns of inter-annual changes of FIS are similar in both reaches (Fig. 4g), which indicates that environmental factors dominate inter-annual change, rather than prey availability. Prey availability may not limit FIS inter-annual changes because FIS have the ability to selectively feed on abundant prey items. On the other hand, FIS production was consistently higher in the fertilized reach than in the reference reach, which indicates that fertilization simulated gross primary production. Although DIA stocks exhibited only minor increase with elevated primary production, total insect abundance (FIS prey) increased with fertilization.

5.3.8. *Comparison between reference and fertilized reach fluxes*

By comparing individual predicted fluxes between the reference and fertilized reaches (Fig. 11), we can infer some overall effects of the fertilization. In general, flux deviations in the fertilized reach exhibit greater dynamics than in the reference reach and changed signs after 1992 when moss cover developed. The predictions indicate that fluxes f_1–f_5 show a decrease for a few years after initiation of fertilization (most notably in 1990; blue arrow in Fig. 11), but then show an increase during the latter phase of the experiment (most notably in 1996; green arrow). Conversely, flows f_7–f_9 exhibit the opposite trends with higher fluxes around 1990 and reduced fluxes around 1996. Base on the flow diagram (Fig. 2), these results suggest that the initial P fertilization caused, surprisingly, a reduction in the autotrophic support for FIS (Fig. 2, red box), but an increased support of FIS growth from the detrital pathways (Fig. 2, blue box). In later years (ca. 1996), the trend reversed, where FIS growth is supported by the autotrophic flow path, and support from the detrital community diminishes.

We know from previous observations that the long-term fertilization caused a dramatic shift in the Kuparuk River food web, with the moss *Hygrohypnum* virtually replacing epilithic diatoms starting in 1992 and reaching sustained high levels in 1996 (Slavik et al., 2004). The change in physical habitat that *Hygrohypnum* provided also resulted in a dramatic increase in CHI abundance, although it does not appear CHI supported FIS growth (Fig. 11f). Interestingly, the dramatic change in food web structure that resulted from the fertilization did not cause a significant change in FIS growth (Fig. 4g and see Slavik et al., 2004). However, our modeling analyses do show that the flow paths of P to FIS did change significantly in the fertilized reach. We speculate that the initial establishment of the moss *Hygrohypnum* in the early 1990s displaced DIA, so that FIS had to rely on the detrital-based pathway via BRA. After moss coverage reached maturity around 1996, FIS return

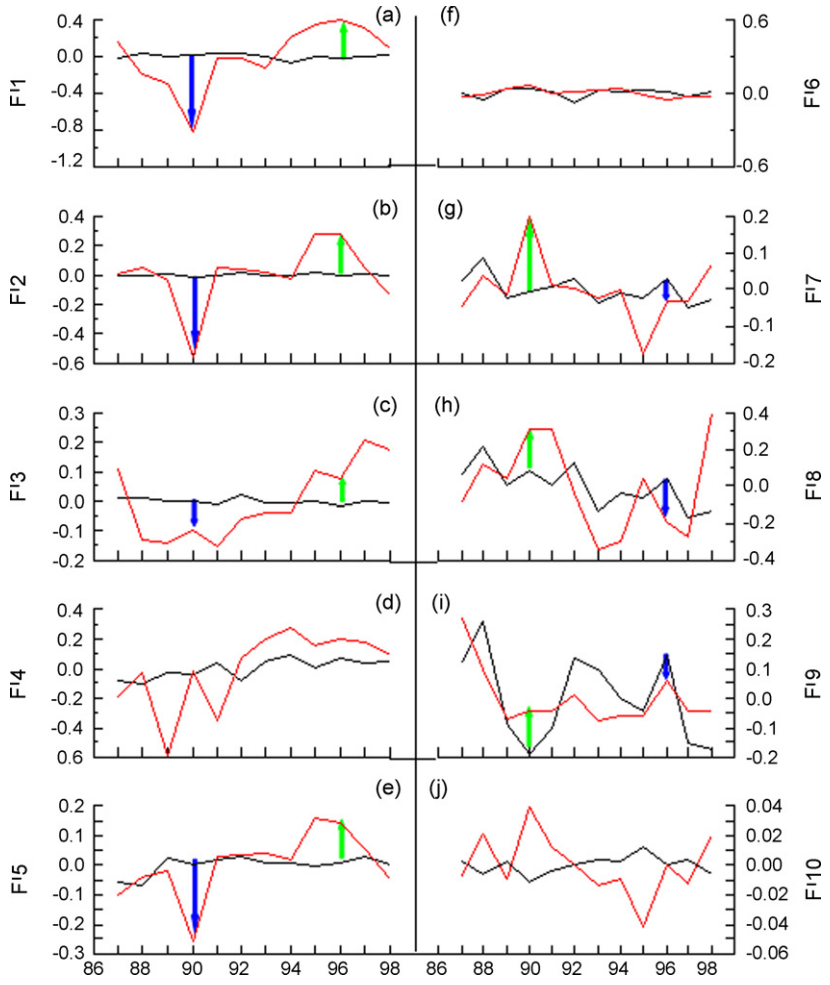

Fig. 11 – Predicted food web model fluxes (mmol P m^{-2} $year^{-1}$) in the reference reach (black lines) as compared to the fertilized reach (red lines). Blue arrows highlight flux decreases in the fertilized reach relative to the reference reach, while green arrows indicate flux increases in the fertilized reach. (For interpretation of the references to colour in this figure legend, the reader is referred to the web version of the article.)

to utilizing the autotrophic-based flow path, perhaps via the mayfly *Ephemerella*, which exhibited large increases in abundance in 1995 (Slavik et al., 2004). Although the mayfly *Baetis* was included in our model (Fig. 2, BAE), *Ephemerella* was not. This lack of inclusion of *Ephemerella* in the model may explain the difficulty in obtaining a good prediction of BAE, but it does illustrate the robustness of the modeling approach to missing data, as we were able to obtain good estimates for the remaining state variables.

6. Conclusion

We have demonstrated how a recently developed inverse model (WV2005) can be used to identify first-order relationships that govern inter-annual dynamics of ecosystem variables in the Kuparuk River ecosystem subject to environmental drivers. Not only does the modeling approach facilitate analysis of whole ecosystem observations, but it can also be used as a long-term forecast model provided projected environmental driver values do not greatly exceed those used during parameter estimation. For example, if the maximum annual temperature observed during parameter estimation was 15 °C then the forecast may be questionable when annual temperatures exceed 15 °C by more than several degrees, which could cause changes in community composition.

The modeling approach is particularly useful when (1) the observations do not encompass the entire food web and (2) the representation of the data is not perfect due to sporadic sampling, large errors, and/or contain measurements that are difficult to quantify or extrapolate to the whole system. Because the modeling approach does not require strict mass balance closure, the model is more robust to such observational uncertainties.

Theoretically, the model approach is only applicable to ecosystem variables that have characteristic times less than 1 year. However, this application shows the approach may be applied to ecosystem variables that violate this requirement provided the annual biomass increment is used and the increment is primarily controlled by the annual environmental drivers, as was the case for FIS in the Kuparuk River ecosystem.

Although FIS growth was not stimulated by fertilization, our model results show that the flow of phosphorous to FIS did switch to detrital-based sources in 1990 following moss recruitment, but then returned to autotrophic-based sources in 1996 as *Ephemerella* replaced the loss of *Baetis* (BAE). This study provides some instruction for improving the observations for future studies in the Kuparuk River. Field observations that should be added in order to improve model performance include: (1) annual mean increment of moss coverage so that it can be included as a state variable; (2) the EPI sloughing mechanism; (3) the relationship between mean annual insect density and river discharge.

Acknowledgements

We are grateful to Dr. Rubao Ji and another anonymous reviewer for their thoughtful comments and constructive suggestions. This research was supported by NSF grant OPP-9911278.

Appendix A

The linear matrix equation is given by

$$AX = \begin{pmatrix} D'_{IP} \\ D'_{IA} \\ B'_{AE} \\ C'_{HI} \\ B'_{RA} \\ B'_{-F} \\ F'_{IS} \end{pmatrix} \tag{A1}$$

where A is a 33×33 matrix with components $a_{i,j}$, where $a_{i,j} = 0$, $\forall i, j \in \{1, 2, \ldots, 33\}$, except,

$$a_{1,1} = -D'_{IP}, \quad a_{1,2} = -D'_{IA}, \quad a_{1,3} = -\frac{\bar{D}_{IP}}{\bar{T}}T', \quad a_{1,4} = -\frac{\bar{D}_{IP}}{\bar{L}}L', \quad a_{1,5} = \alpha D'_{IA}, \quad a_{1,6} = \alpha B'_{AE},$$
$$a_{1,7} = \alpha\frac{\bar{D}_{IA}}{\bar{T}}T', \quad a_{1,8} = -\alpha\frac{\bar{D}_{IA}}{\bar{D}}D',$$

$$a_{1,9} = \alpha D'_{IA}, \quad a_{1,10} = \alpha C'_{HI}, \quad a_{1,11} = \alpha\frac{\bar{D}_{IA}}{\bar{T}}T', \quad a_{1,12} = -\alpha\frac{\bar{D}_{IA}}{\bar{D}}D', \quad a_{1,15} = \alpha B'_{AE}, \quad a_{1,16} = \alpha F'_{IS},$$
$$a_{1,17} = \alpha\frac{\bar{B}_{AE}}{\bar{T}}T', \quad a_{1,18} = \alpha\frac{\bar{B}_{AE}}{\bar{D}}D',$$

$$a_{1,19} = \alpha C'_{HI}, \quad a_{1,20} = \alpha F'_{IS}, \quad a_{1,21} = \alpha\frac{\bar{C}_{HI}}{\bar{T}}T', \quad a_{1,22} = \alpha\frac{\bar{C}_{HI}}{\bar{D}}D', \quad a_{1,23} = \alpha B'_{RA}, \quad a_{1,24} = \alpha F'_{IS},$$
$$a_{1,25} = \alpha\frac{\bar{B}_{RA}}{\bar{T}}T', \quad a_{1,26} = \alpha\frac{\bar{B}_{RA}}{\bar{D}}D',$$

$$a_{1,27} = \alpha B'_{RA}, \quad a_{1,28} = \alpha\frac{\bar{B}_{RA}}{\bar{T}}T', \quad a_{1,29} = \alpha\frac{\bar{B}_{RA}}{\bar{D}}D', \quad a_{1,30} = \alpha B'_{-F}, \quad a_{1,31} = \alpha\frac{\bar{B}_{-F}}{\bar{T}}T', \quad a_{1,32} = \alpha\frac{\bar{B}_{-F}}{\bar{D}}D',$$
$$a_{1,33} = \frac{\bar{D}_{IP}}{\bar{D}}D', \quad a_{2,1} = \beta D'_{IP},$$

$$a_{2,2} = \beta D'_{IA}, \quad a_{2,3} = \beta\frac{\bar{D}_{IP}}{\bar{T}}T', \quad a_{2,4} = \beta\frac{\bar{D}_{IP}}{\bar{L}}L', \quad a_{2,5} = -D'_{IA}, \quad a_{2,6} = -B'_{AE}, \quad a_{2,7} = -\frac{\bar{D}_{IA}}{\bar{T}}T',$$
$$a_{2,8} = \frac{\bar{D}_{IA}}{\bar{D}}D', \quad a_{2,9} = -D'_{IA},$$

$$a_{2,10} = -C'_{HI}, \quad a_{2,11} = -\frac{\bar{D}_{IA}}{\bar{T}}T', \quad a_{2,12} = \frac{\bar{D}_{IA}}{\bar{D}}D', \quad a_{2,13} = -D'_{IA}, \quad a_{2,14} = -\frac{\bar{D}_{IA}}{\bar{D}}D', \quad a_{3,5} = \gamma D'_{IA},$$
$$a_{3,6} = \gamma B'_{AE}, \quad a_{3,7} = \gamma\frac{\bar{D}_{IA}}{\bar{T}}T', \quad a_{3,8} = -\gamma\frac{\bar{D}_{IA}}{\bar{D}}D',$$

$$a_{3,15} = -B'_{AE}, \quad a_{3,16} = -F'_{IS}, \quad a_{3,17} = -\frac{\bar{B}_{AE}}{\bar{T}}T', \quad a_{3,18} = -\frac{\bar{B}_{AE}}{\bar{D}}D', \quad a_{4,9} = \gamma D'_{IA}, \quad a_{4,10} = \gamma C'_{HI},$$
$$a_{4,11} = \gamma\frac{\bar{D}_{IA}}{\bar{T}}T', \quad a_{4,12} = -\gamma\frac{\bar{D}_{IA}}{\bar{D}}D', \quad a_{4,19} = -C'_{HI}, \quad a_{4,20} = -F'_{IS},$$

$$a_{4,21} = -\frac{\bar{C}_{HI}}{\bar{T}}T', \quad a_{4,22} = -\frac{\bar{C}_{HI}}{\bar{D}}D', \quad a_{5,23} = -B'_{RA}, \quad a_{5,24} = -F'_{IS}, \quad a_{5,25} = -\frac{\bar{B}_{RA}}{\bar{T}}T', \quad a_{5,26} = -\frac{\bar{B}_{RA}}{\bar{D}}D',$$
$$a_{5,27} = \gamma B'_{RA}, \quad a_{5,28} = \gamma\frac{\bar{B}_{RA}}{\bar{T}}T',$$

$$a_{5,29} = \gamma\frac{\bar{B}_{RA}}{\bar{D}}D', \quad a_{6,30} = \gamma B'_{-F}, \quad a_{6,31} = \gamma\frac{\bar{B}_{-F}}{\bar{T}}T', \quad a_{6,32} = \gamma\frac{\bar{B}_{-F}}{\bar{D}}D', \quad a_{7,15} = \gamma B'_{AE}, \quad a_{7,16} = \gamma F'_{IS},$$
$$a_{7,17} = \gamma\frac{\bar{B}_{AE}}{\bar{T}}T', \quad a_{7,18} = \gamma\frac{\bar{B}_{AE}}{\bar{D}}D', \quad a_{7,19} = \gamma C'_{HI}, \quad a_{7,20} = \gamma F'_{IS}, \quad a_{7,21} = \gamma\frac{\bar{C}_{HI}}{\bar{T}}T',$$

and X is a 33×1 vector of unknowns,

$$x_1 = c_{11}, \quad x_2 = c_{12}, \quad x_3 = c_{13}, \quad x_4 = c_{14}, \quad x_5 = c_{21}, \quad x_6 = c_{22}, \quad x_7 = c_{23}, \quad x_8 = c_{24}, \quad x_9 = c_{31}, \quad x_{10} = c_{32},$$
$$x_{11} = c_{33}, \quad x_{12} = c_{34},$$
$$x_{13} = c_{41}, \quad x_{14} = c_{42}, \quad x_{15} = c_{51}, \quad x_{16} = c_{52}, \quad x_{17} = c_{53}, \quad x_{18} = c_{54}, \quad x_{19} = c_{61}, \quad x_{20} = c_{62},$$
$$x_{21} = c_{63}, \quad x_{22} = c_{64},$$

$$x_{23} = c_{71}, \quad x_{24} = c_{72}, \quad x_{25} = c_{73}, \quad x_{26} = c_{74},$$

$$x_{27} = c_{81}, \quad x_{28} = c_{82}, \quad x_{29} = c_{83}, \quad x_{30} = c_{91},$$

$$x_{31} = c_{92}, \quad x_{32} = c_{93}, \quad x_{33} = c_{101}$$

The matrix Eq. (A1) can be rearranged to solve for the annual mean increment from the long-term mean values, as given by

$$\begin{pmatrix} -c_{11}-1 & -c_{12}+\alpha(c_{21}+c_{31}+c_{41}) & \alpha(c_{22}+c_{51}) & \alpha(c_{32}+c_{61}) & \alpha(c_{71}+c_{81}) & \alpha c_{91} & \alpha(c_{52}+c_{62}+c_{72}) \\ \beta c_{11} & \beta c_{12}-c_{21}-c_{31}-c_{41}-1 & -c_{22} & -c_{32} & 0 & 0 & 0 \\ 0 & \gamma c_{21} & \gamma c_{22}-c_{51}-1 & 0 & 0 & 0 & -c_{52} \\ 0 & \gamma c_{31} & 0 & \gamma c_{32}-c_{61}-1 & 0 & 0 & -c_{62} \\ 0 & 0 & 0 & 0 & -c_{71}+\gamma c_{81}-1 & 0 & -c_{72} \\ 0 & 0 & 0 & 0 & 0 & \gamma c_{91}-1 & 0 \\ 0 & 0 & \gamma c_{51} & \gamma c_{61} & \gamma c_{71} & 0 & \gamma(c_{52}+c_{62}+c_{72})-1 \end{pmatrix} \begin{pmatrix} D'_{IP} \\ D'_{IA} \\ B'_{AE} \\ C'_{HI} \\ B'_{RA} \\ B'_{-F} \\ F'_{IS} \end{pmatrix} = \begin{pmatrix} -B_1 \\ -B_2 \\ -B_3 \\ -B_4 \\ -B_5 \\ -B_6 \\ -B_7 \end{pmatrix} \quad \text{(A2)}$$

where the B vector is given by

$$B_1 = (-C_{13}\bar{D}_{IP} + \alpha(C_{23}\bar{D}_{IA} + C_{33}\bar{D}_{IA} + C_{53}\bar{B}_{AE} + C_{63}\bar{C}_{HI} + C_{73}\bar{B}_{RA} + C_{82}\bar{B}_{RA} + C_{92}\bar{B}_{-F}))\frac{T'}{\bar{T}} + (\alpha(-C_{24}\bar{D}_{IA} - C_{34}\bar{D}_{IA} + C_{54}\bar{B}_{AE} + C_{64}\bar{C}_{HI} + C_{74}\bar{B}_{RA} + C_{83}\bar{B}_{RA} + C_{93}\bar{B}_{-F}) + C_{101}\bar{D}_{IP})\frac{D'}{\bar{D}} - C_{14}\bar{D}_{IP}\frac{L'}{\bar{L}},$$

$$B_2 = (\beta C_{13}\bar{D}_{IP} - C_{23}\bar{D}_{IA} - C_{33}\bar{D}_{IA})\frac{T'}{\bar{T}} + (C_{24}\bar{D}_{IA} + C_{34}\bar{D}_{IA} - C_{42}\bar{D}_{IA})\frac{D'}{\bar{D}} + \beta C_{14}\bar{D}_{IP}\frac{L'}{\bar{L}},$$

$$B_3 = (\gamma C_{23}\bar{D}_{IA} - C_{53}\bar{B}_{AE})\frac{T'}{\bar{T}} + (-\gamma C_{24}\bar{D}_{IA} - C_{54}\bar{B}_{AE})\frac{D'}{\bar{D}},$$

$$B_4 = (\gamma C_{33}\bar{D}_{IA} - C_{63}\bar{C}_{HI})\frac{T'}{\bar{T}} + (-\gamma C_{34}\bar{D}_{IA} - C_{64}\bar{C}_{HI})\frac{D'}{\bar{D}},$$

$$B_5 = (-C_{73}\bar{B}_{RA} + \gamma C_{82}\bar{B}_{RA})\frac{T'}{\bar{T}} + (-C_{74}\bar{B}_{RA} + \gamma C_{83}\bar{B}_{RA})\frac{D'}{\bar{D}},$$

$$B_6 = \gamma C_{92}\bar{B}_{-F}\frac{T'}{\bar{T}} + \gamma C_{93}\bar{B}_{-F}\frac{D'}{\bar{D}},$$

$$B_7 = \gamma(C_{53}\bar{B}_{AE} + C_{63}\bar{C}_{HI} + C_{73}\bar{B}_{RA})\frac{T'}{\bar{T}} + \gamma(C_{54}\bar{B}_{AE} + C_{64}\bar{C}_{HI}54 + C_{74}\bar{B}_{RA})\frac{D'}{\bar{D}}$$

REFERENCES

Arscott, D.B., Bowden, W.B., Finlay, J.C., 1998. Comparison of epilithic algal and bryophyte metabolism in an Arctic tundra stream, Alaska. J. North Am. Benthol. Soc. 17 (2), 210–227.

Bowden, W.B., Peterson, B.J., Finlay, J.C., et al., 1992. Epilithic chlorophyll a, photosynthesis, and respiration in control and fertilized reaches of a tundra stream. Hydrobiologia 240 (1–3), 121–131.

Bowden, W.B., Finlay, J.C., Maloney, P.E., 1994. Long-term effects of PO_4 fertilization on the distribution of bryophytes in an Arctic river. Freshwater Biol. 32 (2), 445–454.

Deegan, L.A., Peterson, B.J., 1992. Whole-river fertilization stimulates fish production in an Arctic tundra river. Can. J. Fish. Aquat. Sci. 49 (9), 1890–1901.

Deegan, L.A., Peterson, B.J., Golden, H., et al., 1997. Effects of fish density and river fertilization on algal standing stocks, invertebrate communities, and fish production in an Arctic river. Can. J. Fish. Aquat. Sci. 54 (2), 269–283.

Deegan, L.A., Golden, H.E., Harvey, C.J., et al., 1999. Influence of environmental variability on the growth of age-0 and adult Arctic grayling. Trans. Am. Fish. Soc. 128 (6).

Finlay, J.C., Bowden, W.B., 1994. Controls on production of bryophytes in an Arctic tundra stream. Freshwater Biol. 32 (2), 455–466.

Ford, T.E., Walch, M., Mitchell, R., et al., 1989. Microbial film formation on metals in an enriched Arctic river. Biofouling 1 (4), 301–311.

Harvey, C.J., Peterson, B.J., Bowden, W.B., et al., 1998. Biological responses to fertilization of Oksrukuyik Creek, a tundra stream. J. North Am. Benthol. Soc. 17 (2), 190–209.

Hershey, A.E., Hiltner, A.L., Hullar, M.A.J., et al., 1988. Nutrient influence on a stream grazer: *Orthocladius* microcommunities respond to nutrient input. Ecology 69 (5), 1383–1392.

Hershey, A.E., Pastor, J., Peterson, B.J., et al., 1993. Stable isotopes resolve the drift paradox for Baetis mayflies in an Arctic river. Ecology 74 (8), 2315–2325.

Hershey, A.E., Bowden, W.B., Deegan, L.A., Hobbie, J.E., Peterson, B.J., Kipphut, G.W., Kling, G.W., Lock, M.A., Merritt, R.W., Miller, M.C., Vestal, J.R., Schuldt, J.A., 1997. The Kuparuk River: a long-term study of biological and chemical processes in an arctic river. In: Milner, A.M., Oswood, M.W. (Eds.), Freshwaters of Alaska. Springer-Verlag, New York, New York, USA, pp. 107–129.

Hiltner, A.L., Hershey, A.E., 1992. Black fly (Diptera: Simuliidae) response to phosphorus enrichment of an Arctic tundra stream. Hydrobiologia 240 (1–3), 259–265.

Hinterleitner-Anderson, D., Hershey, A.E., Schuldt, J.A., 1992. The effects of river fertilization on mayfly (*Baetis* sp.) drift patterns and population density in an Arctic river. Hydrobiologia 240 (1–3), 247–258.

Hullar, M.A., Vestal, J.R., 1989. The effects of nutrient limitation and stream discharge on the epilithic microbial community in an oligotrophic Arctic stream. Hydrobiologia 172, 19–26.

Hullar, M.A., Vestal, J.R., 1988. The effects of nutrient limitation and stream discharge on the epilithic microbial community in an oligotrophic Arctic stream. In: Proceedings of the Congress in New Zealand 1987, p. 1099.

Kriet, K., Peterson, B.J., Corliss, T.L., 1992. Water and sediment export of the upper Kuparuk River drainage of the North Slope of Alaska. Hydrobiologia 240, 71–81.

Legates, D.R., Mccabe, G.J., 1999. Evaluating the use of "goodness-of-fit" measures in hydrologic and hydroclimatic model validation. Water Resour. Res. 35 (1), 233–241.

Miller, M.C., DeOliveira, P., Gibeau, G.G., 1992. Epilithic diatom community response to years of PO_4 fertilization: Kuparuk River, Alaska (68N Lat.). Hydrobiologia 240 (1–3), 103–119.

Peterson, B.J., Corliss, T., Kriet, K., et al., 1992. Nitrogen and phosphorus concentrations and export for the upper Kuparuk River on the North Slope of Alaska in 1980. Hydrobiologia 240, 61–69.

Peterson, B., Fry, B., Deegan, K., et al., 1993. The trophic significance of epilithic algal production in a fertilized tundra river ecosystem. Limnol. Oceanogr. 38 (4), 872–878.

Rublee, P.A., Partusch-Talley, A., 1995. Microfaunal response to fertilization of an Arctic tundra stream. Freshwater Biol. 34 (1), 81–90.

Slavik, K., Peterson, B.J., Deegan, L.A., Bowden, W.B., Hershey, A.E., Hobbie, J., 2004. Long-term responses of the Kuparuk rive to phosphorus fertilization. Ecology 85 (4), 939–954.
van den Berg, H.A., 1998. Propagation of permanent perturbations in food chains and food webs. Ecol. Model. 107, 225–235.
Wetmore, S.H., Mackay, R.J., Newbury, R.W., 1990. Characterization of the hydraulic habitat of *Brachycentrus occidentalis*, a filter-feeding Caddisfly. J. North Am. Benthol. Soc. 9 (2), 157–169.
Wollheim, W.M., Peterson, B.J., Deegan, L.A., et al., 1999. A coupled field and modeling approach for the analysis of nitrogen cycling in streams. J. North Am. Benthol. Soc. 18 (2), 199–221.
Wollheim, W.M., Peterson, B.J., Deegan, L.A., Hobbie, J.E., Hooker, B., Bowden, W.B., Edwardson, K.J., Arscott, D.B., Hershey, A.E., Finlay, J., 2001. Influence of stream size on ammonium and suspended particulate nitrogen processing. Limnol. Oceanogr. 46 (1), 1–13.
Wan, Z., Vallino, J., 2005. An inverse ecosystem model of year-to-year variations with first order approximation to the annual mean fluxes. Ecol. Model. 187 (4), 369–388.